

# Alkaline-ultramafic lamprophyre dykes from the Vestfold Hills, Princess Elizabeth Land (East Antarctica): primitive magmas of deep mantle origin

C.P.DELOR\* and N.M.S.ROCK

Department of Geology, University of Western Australia, Nedlands WA 6009, Australia

\* Present address: Dept. Cartes et Syntheses, BRGM, Ave. de Concyr, BP6009 Orléans, France

**Abstract:** Alkaline dykes tentatively dated at ~1.3 Ga cut the Vestfold Hills in a consistent N–S to N15°E direction. They form a spectrum between more abundant ultramafic lamprophyres (UML) corresponding broadly to H<sub>2</sub>O–CO<sub>2</sub>-rich nephelinites, and alkaline lamprophyres (AL), representing H<sub>2</sub>O–CO<sub>2</sub>-rich basanites. Olivine (Fo<sub>46-93</sub>, averaging Fo<sub>75</sub>) is abundant only in the UML, but both types carry primary diopsidic clinopyroxene with complex zoning; amphibole (pargasite, hastingsite, kaersutite with up to 8.6% TiO<sub>2</sub>); titanian phlogopite (up to 10% TiO<sub>2</sub>); feldspars (orthoclase, anorthoclase, albite and andesine), nepheline (K-poor and Si-rich), ilmenite (up to 1% MgO and MnO), chrome titanomagnetite, and carbonate (magnesian calcite, ferroan dolomite, breunnerite). Lamprophyric peculiarities include the local coexistence of three feldspars, extremely Ti-rich amphiboles and micas, and the presence of globular structures and possibly primary carbonates. Some dykes carry small but abundant lherzolite xenoliths, others carry chromian diopside (1% Cr<sub>2</sub>O<sub>3</sub>) and En<sub>58-76</sub> orthopyroxene xenocrysts. The dykes represent primitive, mantle-derived magmas which have undergone varying but generally low degrees of polybaric fractionation, together perhaps with mixing of more primitive and fractionated batches, during their ascent through the crust.

Received 1 October 1990, accepted 1 August 1991

**Key words:** alkaline dyke, geochemistry, lamprophyre, mineralogy, petrology

## Introduction

During the last decade, interest in lamprophyric rocks has risen as experimental studies and field associations with kimberlites have emphasized their deep-seated mantle origin. These rocks provide key opportunities to decipher mantle mineralogy and its dynamic processes. Encouraged by major and potential diamond finds, geological survey in Gondwana fragments has greatly increased the number of known kimberlite, lamproite and lamprophyre occurrences (Rock 1991). By contrast, Antarctica remains relatively poorly documented. This is the first detailed account of these particular rocks from the Vestfold Hills, and indeed the first account of Precambrian lamprophyric dykes from Antarctica as a whole. It is also a new addition to the relatively few mantle xenolith localities known so far in Antarctica (cf. Nixon 1987). For brevity, these lamprophyre dykes from the Vestfold Hills will be referred to informally in this paper as the “Vestfold lamprophyres”.

## Geological setting and previous work

The Vestfold Hills (Fig. 1) form an ice free area of c. 400 km<sup>2</sup> on the eastern shore of Prydz Bay. The area has been delineated by James & Tingey (1983) as an Archaean block comprising E–W striking orthogneisses (Mossel gneisses) and paragneisses (Chelnock supracrustals), both dissected

by dense swarms of early to middle Proterozoic mafic dykes. The dominant tholeiitic dykes have been grouped by Collerson & Sheraton (1986) into three generations at 2.4, 1.8 and 1.4 Ga.

These authors also reported “rare alkali basaltic-lamprophyric dykes”, for which they gave four whole-rock analyses and summary petrography, but no mineralogical data. They were thought to postdate the intrusion of anorogenic granites (c. 650–400 Ma), but to predate the separation of Antarctica from India at ~100 Ma. The dykes were not specifically mentioned in a review of Antarctic mafic dykes by Sheraton *et al.* (1987), except in an addendum, where Kuehner (1987) referred very briefly to “alkaline dykes” from the Vestfold Hills. In contrast to Collerson & Sheraton, Kuehner believed these dykes to be Proterozoic (~1.38 Ga), apparently on the basis of mutually cross-cutting relationships (in both senses) with the 1.3 Ga tholeiitic swarms. Kuehner (1986) also presented whole-rock analyses of the dykes, but did not discuss them in the body of his unpublished thesis.

More recent work by Seitz (1990) and Mikhalsky & Andronikov (1990) — so far presented only as brief abstracts — has favoured Kuehner’s Proterozoic interpretation for these lamprophyric dykes, and assigned them to an intrusive episode immediately prior to the 1.3 Ga tholeiitic dykes. Numerous analyses have apparently been made of these rocks, but none has been published, and no probe work has apparently been undertaken at all.

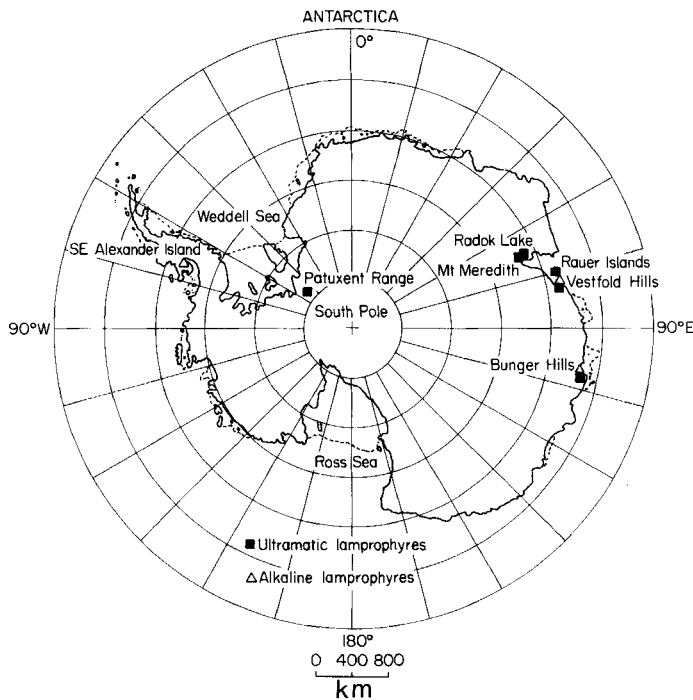


**Fig. 1.** Locality map showing the Vestfold Hills and other known lamprophyric rocks of similar alkaline-ultramafic composition in Antarctica. Localities for lamprophyric rocks of different composition (e.g. lamproites) are omitted for clarity, but are listed and plotted by Rock (1991).

## Field occurrence

### *Dyke morphology and texture*

The lamprophyre dykes vary in width from a few cm to a few metres and show a consistent N10°E to N15°E strike. Coarse-grained examples are characterized in the field by macroscopic biotite, olivine-rich ultramafic xenoliths, or sub-mm scale carbonate-rich ocelli. Finer-grained assemblages have textures very similar to the tholeiites, and it is not always possible to distinguish the two unequivocally at outcrop (especially where their strikes are sub-parallel). Confusion of lamprophyres with N–S trending tholeiites has almost certainly determined the conflicting previous estimates of their age. Chilled margins, restricted to between 2 and 5 cm thickness, are commonly observed, and suggest that lamprophyres were emplaced in a relatively cool basement at supra- to meso-crustal levels. The absence of contact metamorphism or bleaching may be due to the anhydrous character of the surrounding Archaean-early Proterozoic granulites.

### *Carbonate veins and breccias*

These are preferentially associated with coarser grained, more ultramafic lamprophyres. Breccias run along dyke margins and do not exceed a few cm in width. Quartz is

present and locally shows well crystallised sub-pyramidal shapes with a characteristic blue colour. A unique carbonate-rich breccia is associated with one dyke near Wyatt Hut (VHD 115), only a few km from the “carbonatite breccia” mentioned by Collerson & Sheraton (1986). The lamprophyre clasts are angular, and range in size from a few mm to several cm in a light-green calcite-quartz matrix.

These carbonate breccias have been detailed by Hoek (1990), who has interpreted them as tectonic, caused by later seismic slip along the (already solid) dyke margins, with consequent generation of pseudotachylite, dyke decarbonation, and intense fluidization. However, these breccias do seem to be associated only with the lamprophyric dykes, and not with tholeiitic dykes of the same orientation in the same localities.

## Petrography

In thin section, the lamprophyres and associated tholeiites are readily distinguished: the lamprophyres carry alkali feldspar, brown amphibole, biotite, carbonate or nepheline, whereas the tholeiites carry plagioclase phenocrysts or quartzose matrix. Textures also differ.

We restrict the terms phenocryst and xenocryst hereafter to crystals believed to be genuinely cognate or foreign to a host, and use ‘macrocryst’ (Mitchell 1986) as a non-genetic term merely connoting crystals larger in size than their host groundmass, which could be true phenocrysts, xenocrysts or something in between.

Many of the dykes are highly carbonated and oxidized, and some are also rich in secondary quartz veins. The oxidation affects all the mafic minerals and tends to complicate optical identification, since even Fe-poor phases may thereby become almost opaque. Nevertheless, the persistently euhedral character of phenocrysts is usually evident even in fine-grained altered examples, and a flow foliation of the macrocrysts is still commonly detectable in dyke margins. Indeed, an abundance of macrocrysts immediately adjacent to country-rocks in the finest-grained specimens, is evidence that the dykes solidified from crystal-charged magmas.

In thin section, two broad groups of lamprophyre dykes may be distinguished: olivine-rich and olivine-poor (Table I). Inferred xenocrysts in both groups are represented by orthopyroxenes and clinopyroxenes, interpreted as mantle xenocrysts, and quartz, presumably representing disaggregated country-rock fragments. Xenocrysts are not always easily identifiable via thin section textures alone, unless reaction rims are present (as with carbonate-clinoamphibole rims around quartz).

### *Olivine-rich dykes*

Fine-grained examples of this group show abundant, mostly pseudo-hexagonal olivine macrocrysts, commonly

**Table I.** Classification and generalized mineralogy of studied lamprophyre dykes from the Vestfold Hills.

	Ol	Cpx	Am (1°)	Bi	Pl	Af	Ne	Cb†
<i>Ultramafic lamprophyres</i> (olivine-rich Vestfold lamprophyres)*								
Damkjernites	√√	√√	±	√√	x	√	√√	√√
Ouachitites	√√	√√	±	√√	x	x	√	√√
<i>Alkaline lamprophyres</i> (olivine-poor Vestfold lamprophyres)								
Camptonites	√	√√	√√	±	√√	√√	±	±
Sannaïtes	√	√√	√√	±	√√	√√	±	±
√ = rare (accessory) phase √√ = minor phase √√√ = abundant (essential) phase ± = abundance varies x = absent								

\* Mikhalsky & Andronikov (1990) also termed the olivine-poor dykes "camptonites", but their use of the name "monchiquite" (another alkaline lamprophyre) for the olivine-rich dykes is not favoured here, because of their ultrabasic/ultramafic composition.

† Ol = olivine, Cpx = clinopyroxene; Am = amphibole (primary); Bi = biotite; Pl = plagioclase; Af = alkali feldspar; Ne = nepheline; Cb = carbonate

pseudomorphed by carbonate-magnetite-talc-tremolite aggregates, which may develop with increasing alteration into larger carbonate-rich aggregates of much vaguer outline. Clinopyroxene inclusions occur in some olivines. Many grains have undergone strong oxidation, together with reactions with the surrounding groundmass: the more highly birefringent (Fe-rich) grains are largely replaced by dark opaque material, and/or surrounded by semi-radial, fine-grained aggregates of biotite, pale clin amphibole (magnesian-cummingtonite — see below), orthopyroxene and other material too fine to resolve even under a microprobe beam. The olivines are associated with somewhat smaller, subhedral to elongate, zoned clinopyroxenes, many of which again have thick, complete opaque rims. Orthopyroxene cores are occasionally found, as are inclusions of carbonate. Coarser-grained examples of this group have a striking inequigranular texture not unlike that of kimberlite (Mitchell 1986), in which euhedral to anhedral olivine and pyroxene macrocrysts are dispersed in an irregular, carbonated and often heavily veined matrix with conspicuous phlogopite, carbonate, opaques and sometimes minor feldspar or nepheline.

One almost pristine dyke (VHD 96a), has a quite different, aphyric, texture from all the other olivine-rich dykes, although it comprises the same mineral assemblage. Anhedral olivines, together with complexly zoned and intergrown clinopyroxene and brown amphibole, are all poikilitically enclosed by large phlogopite-biotite plates, with minor nepheline forming interstitial pools. It includes large, polycrystalline, dunitic xenolithic aggregates, whose olivine rims show a light-brown secondary staining, contrasting with the colourless xenocryst olivine cores. The olivines have associated

colourless clin amphibole and are irregularly veined by complex clinopyroxene-oxide symplectites. This feature also characterizes numerous small euhedral olivine inclusions observed in some clinopyroxene cores. Such textures indicate that clinopyroxenes are in part phenocrysts which developed from an early olivine-rich paragenesis at a late magmatic stage.

### *Olivine-poor dykes*

These are conspicuously porphyritic, with abundant, panidiomorphic (pseudo-octagonal) clinopyroxene phenocrysts, commonly showing much more complex zoning than in the olivine-rich dykes (including oscillatory and/or sector styles within the same grain), sieve-textured interiors, and glomeroporphyritic or cumulo-phyrlic textures with opaques. Felsic minerals tend to be more concentrated into felsic segregations than in the olivine-rich dykes, and these may in turn develop into better-defined feldspathic globular structures ('ocelli'), which are coarser than the phenocrysts. Such features are characteristic of lamprophyres (Rock 1987, 1991). Other globular structures are filled with combinations of carbonate, pale tremolitic amphibole needles, alkali feldspar, and phlogopite-biotite coarser than the surrounding groundmass, sometimes in texturally complex radiating sheaves. In one dyke (VHD 26), calcite ocelli develop preferentially around biotite and ilmenite nuclei. Ilmenite may also occur around these structures. In the more carbonated dykes, these globular structures may be extremely difficult to tell from carbonate aggregates after olivine phenocrysts.

### **Whole-rock geochemistry**

The freshest available dykes were analysed for major elements and 19 trace elements, along with one inferred contemporaneous tholeiitic dyke for comparison (Table II). Our data appear to be entirely consistent with the four analyses of Collerson & Sheraton (1986) and, insofar as can be determined from their brief abstract, with the data of Mikhalsky & Andronikov (1990). They also appear to represent fully all the alkaline-ultrabasic compositions in a much larger set of analyses of Vestfold lamprophyres made by students at the University of Tasmania (e.g. Kuehner, 1986; M. Seitz, personal communication, 1991).

On the TAS (Total Alkali-Silica) diagram, recommended by the IUGS for the classification of fine-grained rocks (Le Bas *et al.* 1986), the lamprophyres plot variously within the foidite, basanite, basalt and trachybasalt fields, well to the alkaline side of the alkaline-tholeiitic divide (Fig. 2). On the additional IUGS criterion,  $\text{Na}_2\text{O} - 2 < \text{or} > \text{K}_2\text{O}$ , all are 'potassic'. In CIPW normative character (Table II), their alkaline character is clearly confirmed by the presence of *ne* in all analyses. The more Si-poor rocks also carry *lc* ( $\text{KAlSi}_2\text{O}_6$ ) or *ka* ( $\text{KAlSiO}_4$ ). Although sharing a low

Table II. Representative new whole-rock analyses of Vestfold lamprophyres (in order of SiO<sub>2</sub> content).

Sample VHD	Ultramafic lamprophyres Damkjernites					Alkaline lamprophyres Melacamptonite Sannaite		Tholeiite	AL*	UML*
	85a	96a	95b	14	85b	115	83			
SiO <sub>2</sub> %	39.80	39.99	41.03	41.71	41.92	45.02	46.33	48.22	42.5	32.3
Al <sub>2</sub> O <sub>3</sub>	5.70	5.71	8.04	7.25	9.08	9.34	11.81	13.39	13.7	6.7
Fe <sub>2</sub> O <sub>3</sub> (t)	13.56	15.66	14.20	15.38	14.18	13.62	13.25	15.57	12.0	13.6
MgO	18.78	21.13	14.58	13.29	9.57	13.17	8.47	6.87	7.1	15.0
CaO	8.20	9.32	9.92	9.35	9.70	10.15	7.95	10.69	10.3	14.0
Na <sub>2</sub> O	0.53	1.77	2.02	1.74	2.11	1.94	3.04	2.12	3.0	1.0
K <sub>2</sub> O	2.24	1.79	2.14	2.24	2.55	1.44	3.02	0.49	2.0	1.9
LOI	7.79	1.24	4.27	3.62	4.56	0.80	0.93	0.10	3.1	3.5
TiO <sub>2</sub>	2.29	2.64	2.82	4.48	3.49	2.54	3.22	2.12	2.9	3.1
P <sub>2</sub> O <sub>5</sub>	0.56	0.64	0.43	0.49	0.93	0.28	0.98	0.21	0.74	1.0
MnO	0.18	0.20	0.18	0.16	0.18	0.16	0.15	0.23	0.20	0.22
Total	99.63	100.09	99.63	99.71	98.27	98.46	99.15	100.01		
Trace elements (ppm), in order of atomic number										
Sc	23	23	21	23	26	27	17	41	21	20
V	167	188	194	242	236	218	135	357	285	250
Cr	637	757	613	561	415	549	174	218	97	480
Co	76	107	66	86	60	84	64	65	38	75
Ni	790	748	472	514	256	418	247	65	65	430
Cu	57	68	91	84	125	80	67	84	50	65
Zn	135	126	117	146	136	114	161	115	98	112
Rb	58	60	71	62	78	50	89	26	50	65
Sr	741	1019	656	705	1220	452	1529	144	990	950
Y	23	26	20	23	34	22	40	45	31	26
Zr	246	207	228	274	400	170	476	132	313	311
Nb	47	52	59	43	80	44	86	12	101	120
Cs	23	21	18	21	28	16	25	15	2	3
Ba	900	1947	970	1270	1478	890	1530	237	930	1100
La	65	81	46	47	111	32	136	13	66	125
Ce	147	153	97	94	237	72	288	29	120	230
Pb	11	20	9	4	21	6	27	5	7	7
Th	10	10	10	5	17	3	22	7	9	10
CIPW norms†										
ab	0.79	0.00	0.00	5.57	8.44	13.06	18.21	18.20		
or	14.60	0.00	9.29	13.97	16.29	8.82	18.38	2.94		
an	7.23	2.41	6.96	5.65	8.40	12.98	9.95	25.94		
lc	0.00	3.68	3.25	0.00	0.00	0.00	0.00	0.00		
ne	2.25	8.32	9.83	5.40	5.88	2.14	4.49	0.00		
ka	0.00	3.50	0.00	0.00	0.00	0.00	0.00	0.00		
di	26.85	32.57	34.03	32.09	30.06	30.05	19.57	21.89		
hy	0.00	0.00	0.00	0.00	0.00	0.00	0.00	21.37		
ol	38.81	39.39	26.62	23.63	18.11	24.22	17.81	1.67		
mt	3.25	3.49	3.28	3.53	3.33	3.07	2.97	3.43		
il	4.80	5.14	5.69	8.98	7.17	5.00	6.30	4.08		
ap	1.43	1.52	1.06	1.20	2.33	0.67	2.34	0.49		
DI‡	17.64	15.50	22.37	24.94	30.61	24.02	41.08	21.13		
mg	83.3	84.2	80.2	77.4	72.7	79.3	71.6	63.6		

All data courtesy of Dr.R. Chang by conventional Norrish-Hutton XRF methods at Geology Dept., University of WA.

† Analyses recalculated to 100% free of volatiles prior to calculation

# Total Fe partitioned using an oxidation ratio (molecular Fe<sup>3+</sup>/[Fe<sup>2+</sup>+ Fe<sup>3+</sup>]) of 0.3 as calculated for Vestfold alkaline dykes by Collerson and Sheraton (1986)

‡ Thornton-Tuttle differentiation index

\* Global averages of 854 alkaline and 456 ultramafic lamprophyres (Rock 1987,1991)



differentiation index, the tholeiite illustrates its quite distinct chemistry not least in the presence of normative *hy* and in its significantly lower *mg*; it also lies on the tholeiitic side of the alkaline-tholeiitic divide in Fig. 2.

The olivine-rich and olivine-poor groups defined on petrographical grounds can be easily distinguished by their chemistry (e.g. Fig. 3a). As shown by the comparative averages and mineral assemblages in Tables I–II, the olivine-rich group corresponds to Rock's (1986, 1991) ultramafic lamprophyres (UML), which are H<sub>2</sub>O–CO<sub>2</sub>-rich variants of nephelinites and melilitites, and the olivine-poor group to alkaline lamprophyres (AL), which are H<sub>2</sub>O–CO<sub>2</sub>-rich basalts and basanites. More specific rock-names are assigned to individual samples in Tables I–II.

From a matrix of correlation coefficients calculated on all 30 analysed elements, Fig. 3 illustrates some of the most statistically significant element covariations. Incompatible elements (Rb, Y, Zr, Nb, Cs) form positive linear arrays with each other (Fig. 3c,d,e), as do compatible elements (Sc, V, Cr, Co, Ni, Mg—Fig. 3b), while incompatibles and compatibles form somewhat weaker negative correlations (Fig. 3f).

On 'spidergrams' (Fig. 4a,b), the lamprophyres all show strong enrichments in LILE, Th, Ce, Nb, Cr and Ni, combined with near-basaltic levels of Ti, Sc and Y. Such patterns are typical of AL and UML (Rock 1987, 1991), and indeed of alkali basaltic to nephelinitic rocks in general. In many element contents, the two AL appear to bracket the group of UML.

Fig. 4c and Table II show that the lamprophyres are not only substantially lower in SiO<sub>2</sub> and Al<sub>2</sub>O<sub>3</sub> than the tholeiitic dykes, but enormously enriched in Mg, Ni, and in all the incompatible and LIL elements (Ti, P, Rb, Sr, Y, Zr, Nb, Ba, La, Ce, Th): several elements are 1–2 orders of magnitude higher. In addition, negative Nb anomalies apparent in the tholeiites are absent from the lamprophyres (Fig. 4c).

### Mineral chemistry

Representative data from 151 mineral analyses made on 12 lamprophyre dykes are cited in Tables III–VII and plotted in Figs. 5–8.

**Olivines** (Table III). The overall range in 27 analyses from the UML is Fo<sub>46–93</sub>, with an average of Fo<sub>75</sub>. Both the overall range, and the maximum zoning observed in an individual grain (Fo<sub>46–75</sub>), are far wider than hitherto reported from lamprophyres, which normally span Fo<sub>70–90</sub> only (Rock 1987, 1991). CaO, NiO and Cr<sub>2</sub>O<sub>3</sub> contents are mostly near detection limits, with a maximum of 0.5% NiO and 0.13% Cr<sub>2</sub>O<sub>3</sub>.

These olivines are somewhat difficult to interpret. The most Fo-rich olivines (Fo<sub>81–93</sub>) occur in an aggregate (sample VHD96a3), and most probably therefore represent a mantle dunite xenolith. However, they are associated in the margins of this xenolith (and in the rest of the rock) with olivines down

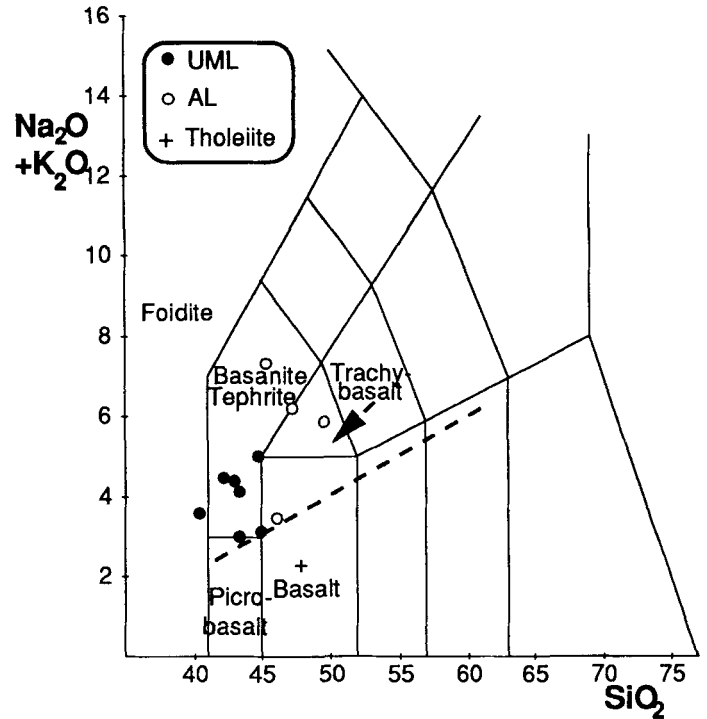
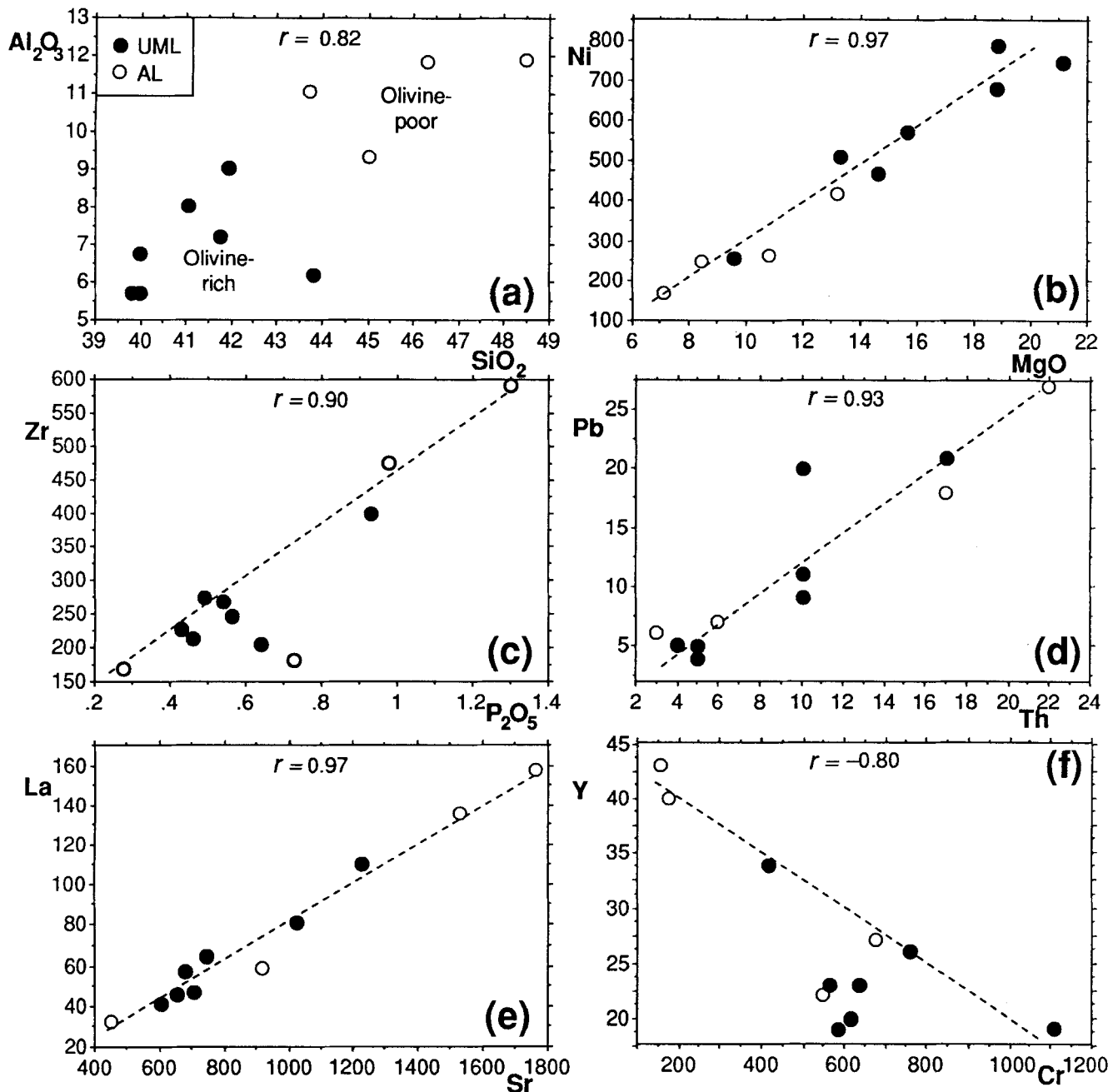


Fig. 2. TAS plot after Le Bas *et al.* (1986) showing position of Vestfold analyses from Table II and from table 6 of Collerson & Sheraton (1986). Analyses recalculated LOI-free before plotting. It should be noted that this diagram is normally recommended only for analyses with < 2% H<sub>2</sub>O and < 0.5% CO<sub>2</sub>. Dashed line is approximate position of alkaline (undersaturated) — tholeiitic (oversaturated) divide.

to Fo<sub>78</sub>, which are too Fe-rich to be mantle xenocrysts. In other dykes, grains with the strongest reaction zones are similarly or even more Fe-rich. Overall, we believe there is a mixture of disaggregated mantle xenocrysts and more Fe-rich cognate phenocrysts in these lamprophyres, both of which have reacted strongly with late-stage volatile-rich fluids. However, as is the case with kimberlites (Mitchell 1986), it is not possible to assign every individual grain to one or other type.

**Orthopyroxenes** (Table VII, Fig. 5a). The overall range in 11 analyses is En<sub>58–76</sub>, and there are three forms of occurrence: (1) in orthopyroxene-oxide-amphibole reaction aggregates around olivines; (2) cores to a few Al-Ti-diopside macrocrysts, and (3) isolated grains replaced by radial-fibrous amphibole material. All these can be assumed xenocrystic, given that the host rocks are *ne*-normative (Table II), and Type 2 appear to have been overgrown by cognate clinopyroxene. Type 1 are more difficult to explain, however, since the reaction should be orthopyroxene-to-olivine in a *ne*-normative magma, not the reverse. The occurrence of En<sub>64–76</sub> orthopyroxene rims to Fo<sub>71–72</sub> olivines in the flow foliated, chilled margin of one dyke (VHD7), suggests contamination by the adjacent quartzo-feldspathic granulite country-rock. However, the



**Fig. 3.** Selected covariations among 12 Vestfold lamprophyres analysed in Table II and by Collerson & Sheraton (1986).  $r$  values are Pearson correlation coefficients; only arrays with  $r > 0.8$ , significant at the 99% level against a null correlation of zero, are plotted. Other paired combinations of K, P, Rb, Y, Nb, Zr, Cs, La, Ce, Th, or of Sc, V, Cr, Co, Ni, Mg, yield similar linear arrays.

occurrence of strongly zoned  $\text{En}_{64-85}$  aggregates around equally strongly zoned ( $\text{Fo}_{46-75}$ ) grains in the interior of another dyke (VHD26a) tends to rule out contamination as a universal explanation, and orthopyroxenes may be connected instead with the intense oxidation of the more Fe-rich olivines.

*Clinopyroxenes* (Table III, Fig. 5). Analyses of 60 clinopyroxenes were made. Those from the UML tend to be slightly more Mg-rich than from the AL, though there is major overlap (Fig. 5a-b). The overall range in the standard

pyroxene quadrilateral is only  $\text{En}_{32-51}\text{Fs}_{3-24}\text{Wo}_{36-50}$  but variations in minor constituents are substantial:  $\text{Al}_2\text{O}_3$  contents range up to 5.2%,  $\text{Na}_2\text{O}$  up to 2%, and  $\text{TiO}_2$  up to 3.2%. Hence the pyroxenes would be described on the IMA (1988) terminology as diopsides or magnesium-rich augites, with the modifiers aluminian, sodian and/or titanian.

Within-grain zoning is highly irregular (Fig. 5b-d). Some grains show virtually no core-rim variations, whereas others even in the same rock show significant but inconsistent

variations in either normal or reverse senses - ie. *mg* can increase or decrease from core-rim (Fig. 5b). If variation in  $\text{Na}_2\text{O}$  is also taken as a measure of pyroxene evolution, even more variants are observable, since most possible combinations of Na varying in the same or opposite sense to *mg* from core  $\rightarrow$  rim or rim  $\rightarrow$  core are observed.

Recognition of xenocrystic clinopyroxenes is obviously more difficult than of orthopyroxene, in such clinopyroxene-rich rocks. However, that occurring as clinopyroxene symplectite (VHD96a: Table VII) is undoubtedly xenocrystic, not only because of its association with xenocrystic olivine, but also because it is a chromian diopside (*sensu* IMA 1988), which occupies different fields from the cognate clinopyroxenes on Fig. 5 due to its lower *mg*,  $\text{Al}_2\text{O}_3$ , and higher  $\text{Cr}_2\text{O}_3$  at low  $\text{TiO}_2$ .

**Amphiboles** (Table IV). Primary amphiboles in the Vestfold lamprophyres are deep brown. On the IMA (1978) nomenclature, nine analyses have the compositions of a varied spectrum of calcic amphiboles (kaersutites, pargasitic, edenitic and hastingsitic hornblendes). One kaersutite (Table IV) has 8.61%  $\text{TiO}_2$ , which is the highest content so far recorded in lamprophyre amphiboles, and among the highest for any natural amphiboles. Secondary amphiboles (mostly associated with alteration of olivine and pyroxene or in reaction rims around quartz xenocrysts) are colourless; eight analyses have magnesio-cummingtonite to actinolite compositions.

**Micas** (Table V, Fig. 6). Nearly all of 21 analyses (mostly small groundmass grains) have phlogopite compositions, with a few straying into the biotite field on Fig. 6a. Most can be expressed as combinations of phlogopite and siderophyllite molecules. Al-poor (tetraferriphlogopite) micas, though common in some other UML (Rock 1986, 1991), were not encountered.  $\text{TiO}_2$  contents range from 2.5–9.9% with an average of 4.9%, the higher values being diagnostic of lamprophyres.  $\text{Na}_2\text{O}$  contents are also notable, reaching 1%. Cl is mostly near detection limits, rising to 0.13%, while  $\text{Cr}_2\text{O}_3$  averages 0.7%, rising to 0.9%. On the few grains large enough to measure core-rim trends, these trends appear to be as irregular and inconsistent in terms of Ti-Al as the clinopyroxene zoning (Fig. 6b), and two of the three sets of data, surprisingly, show lower *mg* in the cores.

**Feldspars** (Table VI, Fig. 7). Three distinct compositional fields were detected in the Vestfold lamprophyres, although as only 10 fresh grains suitable for analysis were located, the possibility cannot be excluded that compositions intermediate between these fields also occur. Assemblages appear to be specific to each dyke: one dyke carries albite ( $\text{Ab}_{90-99}$ ) only (in globular structures with dolomite, or interstitial in the matrix), whereas another carries andesine ( $\text{Ab}_{72-75}$ ) only, and a third has three coexisting feldspars as separate, essentially unzoned, grains (Table VI): anorthoclase ( $\sim\text{Ab}_{50}$ ), orthoclase ( $\sim\text{Or}_{93}$ ) and albite ( $\sim\text{Ab}_{90}$ ). Collerson & Sheraton (1986) mentioned yet another feldspar assemblage in one of their samples: coexisting  $\text{Ab}_{91}$  and  $\text{Ab}_{51}\text{Or}_{41}$ . The mere occurrence

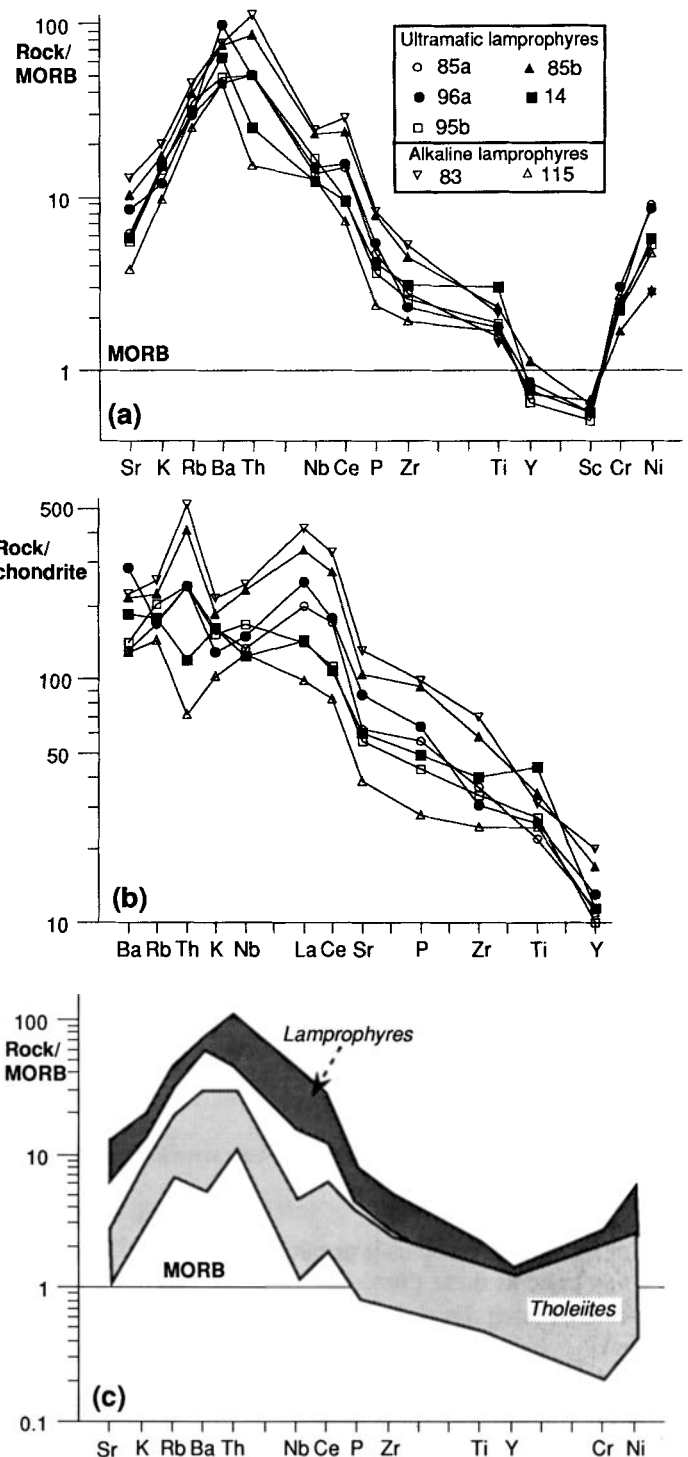


Fig. 4. 'Spidergrams' of Vestfold lamprophyres. a. Lamprophyres normalized to MORB, using Pearce's (1983) element order and normalizing values; b. Lamprophyres normalized to average chondrite, using Thompson's (1982) order and values. Blank tick-marks correspond to elements included by these two authors but not analysed in the present study. c. Field of lamprophyres compared with the field formed by averages for three Proterozoic tholeiitic dyke-suites in the Vestfold Block (Sheraton *et al.* 1987), normalized as in a.

Table III. Representative analyses of cognate ilmenites, spinels, pyroxenes and olivines.

Mineral	Ilmenite	Spinel		Clinopyroxenes				Olivines		
Sample VHD	83	96a	96a	26a	14	85a	114	96a	96a	26a
SiO <sub>2</sub>	0.47	0.20	0.29	48.08	49.52	51.94	53.46	37.49	41.35	38.16
Al <sub>2</sub> O <sub>3</sub>	0.17	1.36	0.62	5.18	4.14	3.88	2.06	*	*	*
FeO	48.36	69.81	87.28	7.20	6.21	8.01	8.47	28.50	10.24	40.94
MgO	0.40	1.45	0.52	13.38	14.33	14.77	15.08	33.28	49.45	19.34
CaO	0.08	*	*	23.13	23.37	18.67	20.39	0.26	bdl	bdl
Na <sub>2</sub> O	0.42	0.63	0.26	0.41	0.17	1.11	0.58	*	*	*
K <sub>2</sub> O	0.11	*	*	0.13	bdl	bdl	0.09	*	*	*
TiO <sub>2</sub>	48.96	5.81	3.73	3.24	2.42	1.03	0.49	*	*	0.15
MnO	1.02	1.29	0.18	bdl	bdl	bdl	0.14	0.71	bdl	0.20
Cr <sub>2</sub> O <sub>3</sub>	bdl	13.81	1.27	0.22	0.53	0.56	0.44	0.13	bdl	bdl
Oxide total	99.99	94.36	94.15	100.97	100.69	99.97	101.20	100.37	101.04	98.78
Formula units										
O =	3	32	32	6	6	6	6	4	4	4
Si	0.012	0.060	0.088	1.772	1.825	1.913	1.955	1.003	1.003	1.092
Al	0.005	0.481	0.221	0.225	0.180	0.168	0.089	*	*	*
Fe <sup>3</sup> §	0.164	9.865	13.753	0.079	0.034	0.011	0.007	*	*	*
Fe <sup>2</sup>	0.841	7.661	8.351	0.143	0.158	0.235	0.252	0.638	0.208	0.980
Mg	0.015	0.649	0.235	0.735	0.787	0.811	0.822	1.328	1.787	0.825
Ca	0.002	*	*	0.914	0.923	0.737	0.799	0.007	0.000	*
Na	0.020	0.367	0.153	0.029	0.012	0.079	0.041	*	*	*
K	0.003	*	*	0.006	0.000	0.000	0.004	*	*	*
Ti	0.916	1.312	0.849	0.090	0.067	0.029	0.013	*	*	*
Mn	0.021	0.328	0.046	0.000	0.000	0.000	0.004	0.016	0.000	0.003
Cr	0.000	3.278	0.304	0.006	0.015	0.016	0.013	0.003	0.000	0.005
Cation total	2.000	24.000	24.000	4.000	4.000	4.000	4.000	2.995	2.997	2.905
New Fe <sub>2</sub> O <sub>3</sub> §	8.78	43.67	60.35	2.86	1.22	0.41	0.24	*	*	*
New FeO	40.46	30.52	32.98	4.62	5.12	7.64	8.25	*	*	*
New %Total	100.87	98.73	100.20	101.25	100.82	100.01	101.22	*	*	*
mg	1.75	7.8	2.7	83.7	83.2	77.5	76.5	67.5	89.5	45.7

§ Ferrous/ferric calculated according to stoichiometry in ilmenite, spinel and pyroxene using the method of Droop (1987)

bdl = analysed but below detection limit

\* = not analysed

All analyses in Tables III–VII were carried out at the Electron Microscopy Centre (UWA) on a ARL microprobe equipped with Energy Dispersive System (EDAX)

of alkali-rich feldspars is peculiar enough for rocks as mafic and basic as these (Table II), especially as these feldspars coexist with Fo-rich olivine, phlogopite and diopsidic clinopyroxene. The coexistence of 2–3 feldspars, including nearly pure Na and K end-members, is even more peculiar in hypabyssal rocks, since this would normally connote slow-cooled, high-pressure subsolvus assemblages. Such features are nevertheless entirely characteristic of lamprophyres and, though far from being well understood, they appear to be connected in some way with the peculiarly volatile-rich nature of the magmas, or the possibly hybrid origin of lamprophyre mineral assemblages (Rock 1987, 1991).

*Nepheline* (Table VI). Two analyses of nepheline have a composition around  $Ne_{75}Ka_{6.8}Qz_{16.18}$  ( $Ne = NaAlSiO_4$ ;  $Ka = KAlSiO_4$ ). They are silicic and K-poor compared with the 'ideal' plutonic (~700°C) Morozewicz composition of around  $Ne_{75}Ka_{20.5}Qz_{4.5}$  (Deer *et al.* 1962), and thus indicate

substantially higher temperatures of crystallization. Two further analyses (not included in Table VI) were even more silicic, corresponding to about  $Ne_{64.70}Ka_{3.7}Qz_{27.29}$  but, because they have a significant excess of Al over [Na+K], it seems likely that these grains lost alkalis in the probe beam.

*Carbonates* (Table V, Fig. 8). There are three quite distinct compositions present among 11 analysed grains and, as with the feldspars, the carbonates vary from dyke to dyke: thus one dyke has a somewhat magnesian calcite; three others have ferroan dolomite (in the latter as inclusions in clinopyroxene), but a fourth has breunnerite [(Mg,Fe)CO<sub>3</sub>]. MnO contents range up to 0.46%, and alkali contents are appreciable (Na<sub>2</sub>O up to 0.38%, K<sub>2</sub>O up to 0.16%). All these compositions have been reported from alkaline or ultramafic lamprophyres (Rock 1987, 1991), but breunnerite in particular is rare in other igneous rocks. Although textural evidence is equivocal, a primary origin for at least some of the carbonate (that not



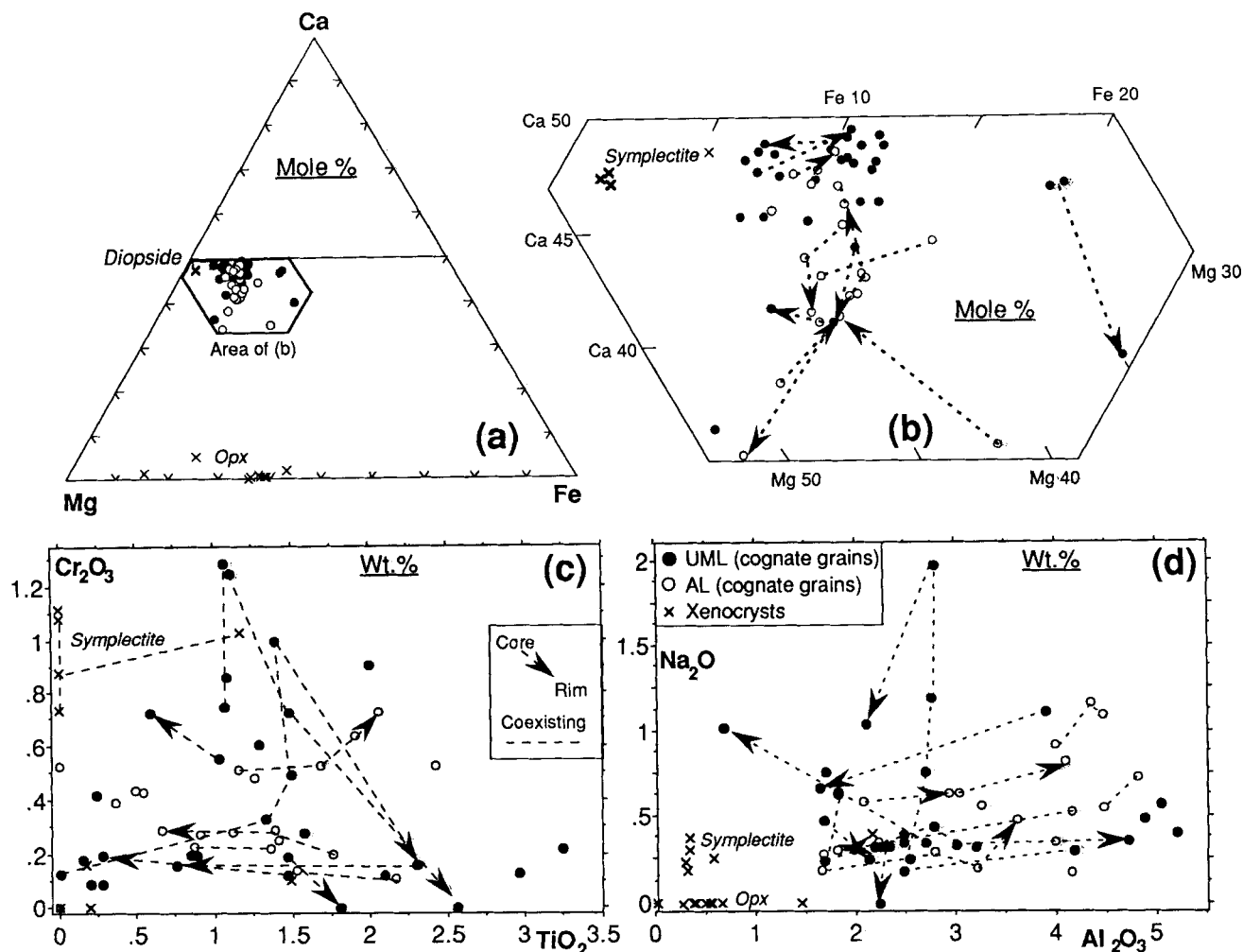


Fig. 5. Plots of pyroxene compositions from Vestfold lamprophyres. Arrowed tie-lines join core-rim traverses across grains; tie-lines without arrows join random spot analyses of single grains. a. Standard pyroxene quadrilateral; b. close-up of a. c. & d. simple bivariate plots to illustrate zoning.

obviously replacing olivine, etc.) seems likely in these rocks. In particular, one sample (VHD 96) shows coarse laths of presumably primary calcite (not ocelli) with acute angles and sharp contacts with co-existing biotite and clinopyroxene phenocrysts.

**Oxides** (Table III). Four analysed ilmenites are normal compositions, with up to 1.3% MgO and 1.0% MnO. Such compositions are typical of basaltic rocks, including many lamprophyres (Rock 1987, 1991). Among six spinel analyses, five proved to be magnetites (up to 1.55%  $\text{Cr}_2\text{O}_3$ , 0.2–8.3%  $\text{TiO}_2$ , 84–92% FeO), whereas the sixth (Table III) is a chromian titanian magnetite.

### Petrogenesis

A detailed discussion of lamprophyre petrogenesis was published by Rock (1991) and, since much of that discussion can be applied to these Vestfold lamprophyres, which are

fairly typical of alkaline and ultramafic lamprophyres elsewhere, only a brief outline is given here.

The Vestfold lamprophyres have *mg* numbers, Sc, Cr, Co and Ni contents which are within most authors' accepted ranges for 'primary' magmas (e.g. Frey *et al.* 1978, Rhodes 1981), although minor accumulation of mafic minerals may have taken place in some dykes (e.g. VHD96a: Table II). Given their bulk chemical similarity to nephelinites, and the presence of orthopyroxene and chromian diopside xenocrysts, there can be little doubt that they originated by low degrees of partial melting of mantle peridotite source at depths much greater than the spatially associated tholeiites.

The LILE enrichments shown on Fig. 4 are common to most alkaline mafic-ultramafic rocks, though very marked in lamprophyres, and introduce problems in that the degrees of melting required to explain the major element compositions would not be expected to generate such extreme LILE enrichments (e.g. Frey *et al.* 1978). Popular ways around this

Table IV. Representative microprobe analyses of cognate amphiboles†.

	Primary calcic amphiboles					Secondary calcic and Mg-Fe-Mn amphiboles				
Sample VHD	115	115	115	96a	96a	6§	83¶	26a*	96a3φ	85aΔ
SiO <sub>2</sub>	39.87	40.21	43.68	45.77	44.70	55.87	40.78	44.06	57.22	56.55
Al <sub>2</sub> O <sub>3</sub>	9.44	9.87	11.85	7.76	8.26	0.56	0.19	bdl	0.22	bdl
FeO	14.72	15.41	12.43	10.49	10.28	9.75	40.68	27.99	4.14	17.07
MgO	11.38	12.77	12.60	15.40	16.78	18.48	15.10	24.43	35.29	22.99
CaO	11.01	10.54	12.26	9.69	8.99	12.06	0.23	0.09	0.22	0.48
Na <sub>2</sub> O	1.43	2.05	2.01	4.62	3.93	0.34	bdl	bdl	bdl	bdl
K <sub>2</sub> O	0.79	0.75	1.07	0.88	0.73	0.13	bdl	bdl	bdl	bdl
TiO <sub>2</sub>	6.42	8.61	2.15	3.46	2.98	bdl	0.30	bdl	bdl	bdl
MnO	0.11	0.19	bdl	bdl	0.15	0.22	0.82	0.18	bdl	bdl
Cr <sub>2</sub> O <sub>3</sub>	bdl	bdl	bdl	0.17	0.09	bdl	bdl	0.08	bdl	bdl
Oxide total	95.17	100.40	98.05	98.24	96.89	97.41	98.10	96.83	97.09	97.25
Cations per formula unit (O = 23)										
Si	6.083	5.781	6.419	6.656	6.421	7.858	6.126	6.334	7.612	8.014
Al	1.699	1.674	2.054	1.331	1.400	.093	.034	.000	.035	.000
Fe <sup>3+</sup> †	.485	.945	.000	.095	1.109	.440	3.993	3.363	.460	.000
Fe <sup>2+</sup>	1.393	.907	1.527	1.180	.125	.706	1.115	.000	.000	2.022
Mg	2.589	2.738	2.761	3.340	3.595	3.876	3.383	5.238	7.002	4.859
Ca	1.800	1.624	1.930	1.510	1.383	1.817	.037	.014	.031	.073
Na	.423	.571	.573	1.303	1.094	.093	.000	.000	.000	.000
K	.154	.138	.201	.163	.134	.023	.000	.000	.000	.000
Ti	.737	.931	.238	.378	.322	.000	.034	.000	.000	.000
Mn	.014	.023	.000	.000	.018	.026	.104	.022	.000	.019
Cr	.000	.000	.000	.020	.010	.000	.000	.009	.000	.000
Cation total	15.377	15.332	15.703	15.976	15.611	14.932	14.826	14.980	15.140	14.987
IMA(1978) classification parameters										
{Ca+Na}B	2.000	2.000	2.000	2.000	2.000	1.910	.037	.014	.031	.073
NaB	.200	.376	.070	.490	.617	.093	.000	.000	.000	.000
{Na+K}A	.376	.333	.703	.975	.612	.023	.000	.000	.000	.000
AlVI	.000	.000	.473	.000	.000	.000	.000	.000	.000	.000
Mg/(Mg+Fe)	.650	.751	.644	.739	.966	.846	.752	1.000	1.000	.706
	Kaersutite	Ferrian Kaersutite	Ferroan Pargasitic Hornblende	Titanian Sodian Edenitic	Titanian Subcalcic Sodian	Actinolite	Ferri-Magnesian-Cummingtonites			
			Hornblende	Hornblende	Magnesian- Hastingsitic Hornblende					

† Analyses recalculated and classified according to IMA (1978) nomenclature using a computer program (Rock & Leake 1984), which attempts to allocate total Fe to Fe<sup>3+</sup> and Fe<sup>2+</sup> to fulfill site occupancy considerations.

φ Pool within polycrystalline olivine aggregate

¶ Alteration product after clinopyroxene

\* In reaction products around Fo<sub>n</sub> olivine grain

§ In olivine pseudomorph

Δ In reaction rim around xenocrystic quartz

include the invocation of:

- (1) mantle source which had been previously enriched in the necessary elements via ancient metasomatism,
- (2) retention of residual garnet (so retaining high La and Ce relative to Y);
- (3) wall-rock interaction;
- (4) very low degrees of partial melting.

The trace element behaviour described earlier provides a *prima facie* case for the consanguinity of the lamprophyres. However, Fig. 3 is not consistent with any simple fractionation relationship between the AL and UML. For example, even though the AL dykes have higher SiO<sub>2</sub> contents and more

Fe-rich micas than the UML (Figs. 3a, 6a), the two are intermingled on Figs. 3b–f and 5a–b. Moreover, the analysed tholeiite in Table II mostly lies on extensions of the 'trends' on Fig. 3, so given the strikingly different spidergram patterns in Fig. 4c, the 'trends' themselves cannot be taken as unequivocal evidence for fractionation.

Complex mineral zoning patterns similar to those in Figs. 5–6 have now been documented in great detail from micas and pyroxenes in numerous lamprophyre occurrences (e.g. Brooks & Printzlau 1978, Scott 1980, Dessai *et al.* 1990), and these authors' descriptions can probably be applied almost wholesale to the Vestfold lamprophyres. The irregular juxtaposition in one dyke of different grains with

Table V. Representative microprobe analyses of cognate micas (in order of increasing TiO<sub>2</sub> content) and of carbonates.

Sample VHD	Micas				Carbonates				
	14	115	115	96a	83	14	96a	115	115
SiO <sub>2</sub>	36.91	36.54	37.67	34.13	0.59	0.48	1.43	0.33	0.42
Al <sub>2</sub> O <sub>3</sub>	14.94	13.99	14.12	14.13	0.11	0.09	bdl	0.14	0.19
FeO	13.33	13.89	13.11	11.09	4.63	5.56	0.83	32.61	31.44
MgO	15.89	14.92	15.15	17.26	18.80	18.29	2.23	21.82	22.71
CaO	*	*	*	*	31.03	29.94	53.99	0.10	0.14
Na <sub>2</sub> O	0.17	0.26	bdl	0.92	bdl	0.23	0.18	0.38	0.28
K <sub>2</sub> O	9.61	9.15	9.09	7.70	0.09	0.13	0.15	bdl	bdl
TiO <sub>2</sub>	3.93	4.95	5.23	9.93	*	*	*	*	*
MnO	*	*	*	*	0.17	0.16	0.12	0.46	0.42
Cl	0.05	bdl	bdl	bdl	*	*	*	*	*
Cr <sub>2</sub> O <sub>3</sub>	bdl	bdl	bdl	bdl	*	*	*	*	*
Oxide total	94.84	93.70	94.37	95.16	*	*	*	*	*
O =	22	22	22	22	3	3	3	3	3
Si	5.515	5.536	5.618	5.040	0.027	0.022	0.066	0.016	0.020
Al	2.631	2.498	2.482	2.459	0.006	0.005	0.000	0.008	0.011
Fe <sup>2</sup>	1.666	1.760	1.635	1.370	0.174	0.213	0.032	1.329	1.270
Mg	3.540	3.370	3.368	3.800	1.260	1.248	0.153	1.585	1.635
Ca	*	*	*	*	1.495	1.468	2.666	0.005	0.007
Na	0.049	0.076	0.000	0.263	0.000	0.020	0.016	0.036	0.026
K	1.832	1.769	1.729	1.451	0.005	0.008	0.009	0.000	0.000
Ti	0.442	0.564	0.587	1.103	*	*	*	*	*
Mn	*	*	*	*	0.006	0.006	0.005	0.019	0.017
Cl	0.013	0.000	0.000	0.000	*	*	*	*	*
Cr	0.000	0.000	0.000	0.000	*	*	*	*	*
Cation total	15.687	15.573	15.419	15.485	2.973	2.990	2.947	2.998	2.987
					Dolomites		Calcite	Breunnerites	

little zoning, or with normal, reverse, inverse, sector, oscillatory or irregular zoning, is considered to reflect polybaric crystallization as magma rose through the crust - although the possibility of disequilibrium crystallization must also always be borne in mind. Pressure will strongly affect the solubility of Al and Ti in all the mafic phases, and the incorporation of minor elements will also be substantially affected by kinetic effects (slow versus rapid cooling rates), and by the compositions of coprecipitates. Crystallization of the high-Ti Vestfold lamprophyre micas and amphiboles, for example, presumably led to core-rim decrease of both Ti and Al in any pyroxene coprecipitates, whereas, if no mica or amphibole had crystallized, Al and Ti might both have increased in the pyroxene. Mixing of somewhat fractionated batches of magma with more primitive magma from below may also explain the reverse and oscillatory zoning observed. These more fractionated melts are represented by whole-rock analysis D of Collerson & Sheraton (1986), which has lower mg, Co and Ni than the present analyses.

Combining the whole-rock and mineral chemistry therefore

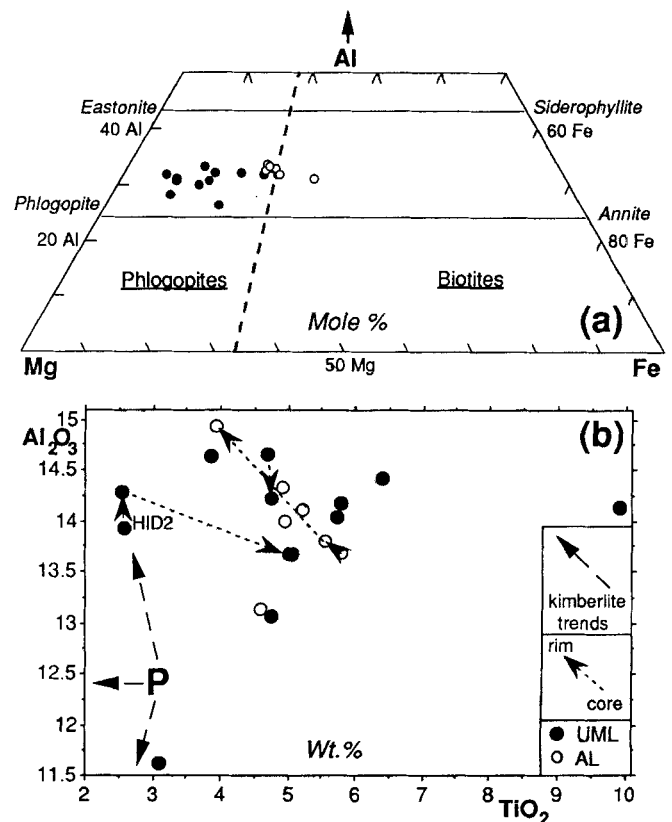


Fig. 6. Plots of mica compositions from Vestfold lamprophyres. a. Standard classification plot after Deer *et al.* (1962). b. Simple bivariate plot to illustrate zoning; P represents typical core compositions of many kimberlite and lamprophyre micas and arrows show resulting evolutionary core-rim trends for kimberlites (after Mitchell 1986, fig. 6.34).

Table VI. Representative microprobe analyses of cognate feldspars and nephelines (in order of increasing Na<sub>2</sub>O content).

Sample VHD	Feldspars							Nephelines	
	83	83	83	115	14	14	14	96a	96a
SiO <sub>2</sub>	65.55	65.84	67.69	61.89	69.08	68.53	70.60	47.60	46.60
Al <sub>2</sub> O <sub>3</sub>	18.12	19.44	20.91	23.97	21.36	20.57	19.57	34.28	33.25
FeO	0.17	bdl	0.16	0.17	bdl	bdl	0.19	0.21	bdl
MgO	bdl	bdl	bdl	0.11	0.18	bdl	0.20	0.19	bdl
CaO	bdl	0.74	1.65	5.76	1.62	1.07	bdl	bdl	0.09
Na <sub>2</sub> O	0.71	5.24	10.12	7.96	10.26	10.51	11.40	15.79	18.08
K <sub>2</sub> O	14.56	8.16	0.38	0.27	0.18	0.18	0.11	2.52	2.26
TiO <sub>2</sub>	bdl	0.11	bdl	bdl	bdl	bdl	bdl	*	*
Cl	*	*	*	*	*	0.31	*	*	*
Oxide total	99.11	99.53	100.91	100.13	102.68	101.10	102.07	100.59	100.28
O =	8	8	8	8	8	8	8	16	16
Si	3.027	2.971	2.938	2.741	2.940	2.970	3.014	4.398	4.359
Al	0.986	1.034	1.070	1.251	1.071	1.051	0.985	3.733	3.666
Fe	0.007	0.000	0.006	0.006	0.000	0.000	0.007	0.016	0.000
Mg	0.000	0.000	0.000	0.007	0.011	0.000	0.013	0.026	0.000
Ca	0.000	0.036	0.077	0.273	0.074	0.050	0.000	0.000	0.009
Na	0.064	0.458	0.852	0.683	0.847	0.883	0.944	2.829	3.279
K	0.858	0.470	0.021	0.015	0.010	0.010	0.006	0.297	0.270
Ti	0.000	0.004	0.000	0.000	0.000	0.000	0.000	*	*
Cl	0.000	0.000	0.000	0.000	0.000	0.023	0.000	*	*
Cation total	4.941	4.972	4.963	4.977	4.953	4.986	4.968	11.299	11.583
Ab,%	7	48	90	70	91	94	99		
An,%	0	3	8	28	8	5	0		
Or,%	93	49	1	2	1	1	1		

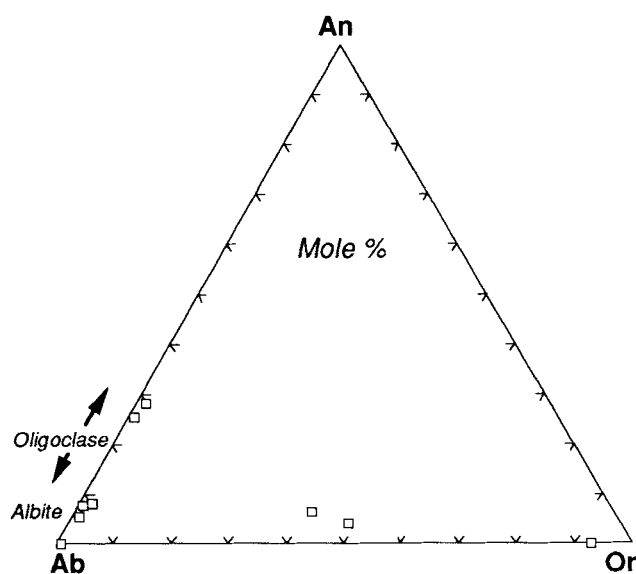


Fig. 7. Plot of feldspar compositions (mole %) from Vestfold lamprophyres.

suggests that the Vestfold lamprophyres represent a continuum of parent magmas, rather than one differentiated parent magma, and that the continuum was derived by melting of the same mantle source under slightly varying conditions. The AL probably reflect slightly larger melt fractions, lower depths or higher  $f\text{CO}_2$  during partial melting,

and have probably experienced slightly more fractionation than the UML during ascent through the crust. Neither group of dykes appears to have suffered significant crustal contamination.

### Regional comparisons

Lamprophyric rocks of a variety of ages and types have now been recognized in Antarctica (Rock 1991), though several as yet remain undescribed in detail. Fig. 1 locates those of most similar composition to the Vestfold lamprophyres. The closest occurrence both geographically and compositionally (though perhaps not in age) is of 'kimberlitic' (?UML) dykes from the Rauer Islands. These are macrocrystic, highly altered and contain xenoliths of talc-serpentine after olivines, spinel and rarely preserved chromian pyrope (authors' unpublished data). Their age relationship to the Vestfold lamprophyres is uncertain.

Another major occurrence of UML is a swarm of Cretaceous (~110 Ma) dykes at Radok (Beaver) Lake, Mac Robertson Land (Ravich *et al.* 1985), with further as yet undescribed examples nearby at Mount Meredith. These occurrences are chemically similar to, but much younger than, the Vestfold lamprophyres (Kuehner 1987).

The other main occurrence of AL is on Alexander Island (Fig. 1), where five isolated camptonite dykes occur in an area otherwise almost free of dykes (Horne & Thomson



Table VII. Representative microprobe analyses of inferred xenocrysts.

Sample VHD	Orthopyroxenes						Clinopyroxenes	
	7¶	7¶	26a¶	26a¶	83*	115Δ	96a#	96a#
SiO <sub>2</sub>	55.50	50.23	51.85	57.50	51.71	53.11	55.40	51.98
Al <sub>2</sub> O <sub>3</sub>	0.56	bdl	bdl	0.37	1.44	.39	0.29	2.14
FeO	14.72	24.43	23.21	9.80	25.81	23.52	1.49	3.28
MgO	26.00	24.83	23.51	32.32	19.33	21.33	18.19	16.00
CaO	2.64	0.10	0.20	0.71	0.96	0.27	23.71	23.38
Na <sub>2</sub> O	0.26	bdl	bdl	bdl	bdl	bdl	0.23	0.40
K <sub>2</sub> O	0.06	bdl	bdl	bdl	0.06	bdl	0.10	bdl
TiO <sub>2</sub>	bdl	bdl	1.49	0.19	0.17	bdl	bdl	1.17
MnO	0.32	0.33	0.42	bdl	0.92	.52	bdl	bdl
Cr <sub>2</sub> O <sub>3</sub>	bdl	bdl	0.10	bdl	0.16	bdl	1.08	1.03
Oxide total	100.06	99.92	100.78	100.89	100.56	99.53	100.49	99.38
O=	6	6	6	6	6	6	6	6
Si	2.001	1.860	1.920	1.993	1.952	1.999	1.995	1.914
Al	0.024	0.000	0.000	0.015	0.064	0.017	0.012	0.093
Fe <sup>3</sup> §	*	0.281	0.076	*	0.020	*	*	0.012
Fe <sup>2</sup>	0.444+	0.475	0.642	0.284+	0.795	0.753+	0.045+	0.089
Mg	1.397	1.370	1.297	1.670	1.088	1.197	0.976	0.878
Ca	0.102	0.004	0.008	0.026	0.039	0.011	0.915	0.923
Na	0.018	0.000	0.000	0.000	0.000	0.000	0.016	0.029
K	0.003	0.000	0.000	0.000	0.003	0.000	0.005	0.000
Ti	0.000	0.000	0.041	0.005	0.005	0.000	0.000	0.032
Mn	0.010	0.010	0.013	0.000	0.029	0.017	0.000	0.000
Cr	0.000	0.000	0.003	0.000	0.005	0.000	0.031	0.030
Cation total	3.999	4.000	4.000	3.993	4.000	3.994	3.995	4.000
New Fe <sub>2</sub> O <sub>3</sub>	*	10.10	2.74	*	0.70	2.37	*	0.45
New FeO	*	15.34	20.75	*	25.18	22.83	*	2.88
New %total	*	100.93	101.05	*	100.63	*	*	99.42
En,%	71.9	74.1	66.6	84.3	56.6	61.0	50.4	46.5
Fs,%	22.8	25.7	33.0	14.3	41.4	38.4	2.3	4.7
Wo,%	5.2	0.2	0.4	1.3	2.0	0.6	47.3	48.8
mg	76.0	74.3	66.9	85.5	57.8	61.4	95.6	90.8

§ Ferrous/ferric calculated according to stoichiometry using the method of Droop (1987)

+ Fe reallocation impossible: calculated cation total < ideal cation total with all Fe as FeO

\* Overgrown by assumed cognate Al-Ti-diopside

Δ Isolated xenocrysts

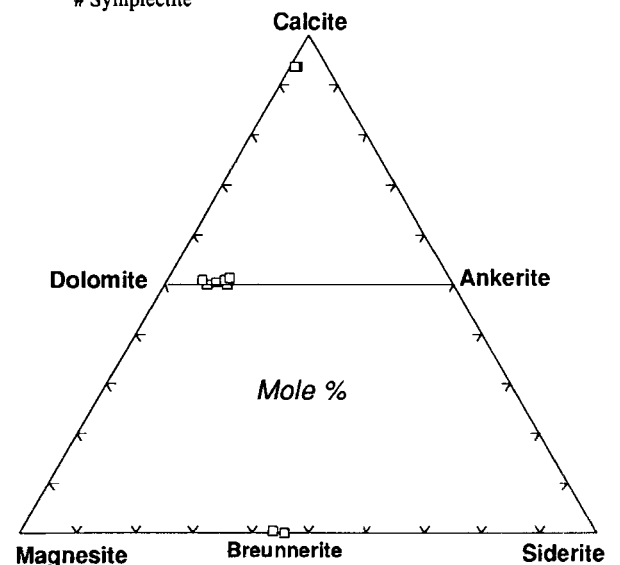
¶ In fine-grained aggregate around olivine macrocryst

# Symplectite

1967). These, too, are much younger, namely Tertiary (~15 Ma).

Reconstructions of Gondwanaland would place the Vestfold area more-or-less coterminous with the Calcutta area of India (see fig.15 of Collerson & Sheraton 1986), where there are large numbers of Cretaceous (105–120 Ma) lamproite sills in the Gondwana coalfields (Rock & Paul 1989, Rock 1991). However, these rocks are substantially more potassic than the Vestfold lamprophyres (carrying K-richrichterite, priderite and perhaps leucite), even though they show similarly high contents of olivine, pyroxene and phlogopite. Lamprophyres from eastern India, which are more similar to the Vestfold

Fig. 8. Plot of carbonate compositions (mole %) from Vestfold lamprophyres.



lamprophyres in composition, include AL swarms around Elchuru in Andhra Pradesh, and from the Garo/Khasi Hills in Meghalaya (Rock & Paul 1989, Rock 1991). More detailed correlation between Antarctica and India must, however, await unequivocal geochronological data.

### Acknowledgements

C.P.D. conducted fieldwork in early 1988, while a member of the Australian National Antarctic Expedition. We thank Ray Chang (UWA) for the analytical results and staff of the UWA EM Centre for assistance with the probe work. John Sheraton kindly commented on the draft manuscript, and drew our attention to hitherto unpublicized occurrences of alkaline dykes in Antarctica.

### References

- BROOKS, C.K. & PRINTZLAU, I. 1978. Magma mixing in alkaline volcanic rocks: the evidence from relict phenocryst phases and other inclusions. *Journal of Volcanology and Geothermal Research*, **4**, 315-331.
- COLLERSON, K.C. & SHERATON, J.W. 1986. Age and geochemical characteristics of a mafic dyke swarm in the Archaean Vestfold block, Antarctica: inferences about Proterozoic dyke emplacement in Gondwana. *Journal of Petrology*, **27**, 853-886.
- DEER, W.A., HOWIE, R.A. & ZUSSMAN, J. 1962. *Rock-forming minerals*. Vol. 3 Sheet silicates. London: Longmans, 270pp.
- DESSAI, A.G., ROCK, N.M.S., GRIFFIN, B.J. & GUPTA, D. 1990. Mineralogy and petrology of some xenolith-bearing alkaline dykes associated with Deccan magmatism, south of Bombay, India. *European Journal of Mineralogy*, **2**, 667-685.
- DROOP, G.T. 1987. A general equation for estimating Fe<sup>3+</sup> concentrations in ferromagnesian silicates and oxides from microprobe analyses, using stoichiometric criteria. *Mineralogical Magazine*, **51**, 43-435.
- FREY, F.A., GREEN, D.H. & ROY, S.D. 1978. Integrated models of basalt petrogenesis: a study of quartz tholeiites to olivine melilitites from south eastern Australia utilizing geochemical and experimental petrological data. *Journal of Petrology*, **19**, 463-513.
- HOEK, J.D. 1990. The emplacement mechanism of carbonate breccia dykes. *Abstract Series Geological Society of Australia*, No. 28 (unpaginated).
- HORNE R.R. & THOMSON, M.R.A. 1967. Post-Aptian camptonite dykes in south-east Alexander Island. *British Antarctic Survey Bulletin*, No. 14, 15-24.
- IMA. 1978. Nomenclature of amphiboles. *Mineralogical Magazine*, **42**, 533-563.
- IMA. 1988. Nomenclature of pyroxenes. *Mineralogical Magazine*, **52**, 535-550.
- JAMES, P.R. & TINGEY, R.J. 1983. The Precambrian evolution of the East Antarctic metamorphic shield - a review. In OLIVER, R.L., JAMES, P.R. & JAGO, J.B. eds. *Antarctic earth science*. Canberra: Australian Academy of Science & Cambridge: Cambridge University Press, 5-10.
- KUEHNER, S.M. 1986. *Mafic dykes of the east Antarctic shield: experimental, geochemical and petrological studies focusing on the Proterozoic evolution of the crust and mantle*. Ph.D thesis, University of Tasmania. [Unpublished].
- KUEHNER, S.M. 1987. Mafic dykes of the East Antarctic Shield: a note on the Vestfold Hills and Mawson Coast occurrences. In HALLS, H.C. & FAHRIG, W.F., eds. *Mafic dyke swarms*. Special Paper Geological Association of Canada, No. 34, 428-429.
- LE BAS, M.J., LE MAITRE, R.W., STRECKEISEN, A. & ZANETTIN, A. 1986. A chemical classification of volcanic rocks based on the total alkali silica diagram. *Journal of Petrology*, **27**, 745-750.
- MIKHALSKY, E.V. & ANDRONIKOV, A.V. 1990. Petrology of late Proterozoic alkaline lamprophyres of Vestfold block, East Antarctica. *Abstract Series Geological Society of Australia*, No. 28 (unpaginated).
- MITCHELL, R.H. 1986. *Kimberlites*. New York: Plenum, 442 pp.
- NIXON, P.H. 1987. *Mantle Xenoliths*. New York: Wiley, 844 pp.
- PEARCE, J.A. 1983. Role of the subcontinental lithosphere in magma genesis at active continental margins. In HAWKESWORTH, C.J. & NORRY, M.J. eds. *Continental basalts and mantle xenoliths*. Orpington: Shiva, 230-249.
- RAVICH, M.G., SOLOV'EV, D.S. & FEDEROV, L.V. 1985. Russian Translation Series, No.24. *Geological structure of Mac.Robertson Land*. Rotterdam: Balkema, 247 pp.
- RHODES, J.M. 1981. Characteristics of primary basalt magmas. In ANON, eds. *Basaltic volcanism on the terrestrial planets*. Oxford: Pergamon, 409-452.
- ROCK, N.M.S. 1986. The nature and origin of ultramafic lamprophyres: aenôites and allied rocks. *Journal of Petrology*, **27**, 155-196.
- ROCK, N.M.S. 1987. The nature and origin of lamprophyres: an overview. In FITTON, J.G. & UPTON, B.G.J., eds. *Alkaline igneous rocks*. Special Publication of the Geological Society of London, No. 30, 191-227.
- ROCK, N.M.S. 1991. *Lamprophyres*. Glasgow: Blackie, 285pp.
- ROCK, N.M.S. & LEAKE, B.E. 1984. The IMA amphibole nomenclature scheme: computerization and its consequences. *Mineralogical Magazine*, **48**, 211-227.
- ROCK, N.M.S. & PAUL, D.K. 1989. 'Kimberlites', 'lamproites' and 'lamprophyres' of India: a bibliography and preliminary reappraisal. *Memoirs of the Geological Society of India*, **15**, 291-311.
- SEITZ, M. 1990. Mafic dykes in the Vestfold Hills - East Antarctica shield. *Abstract Series Geological Society of Australia*, No. 28 (unpaginated).
- SCOTT, P.W. 1980. Zoned pyroxenes and amphiboles from camptonites near Gran, Oslo region, Norway. *Mineralogical Magazine*, **43**, 913-917.
- SHERATON, J.W., THOMSON, J.W. & COLLERSON, K.D. 1987. Mafic dyke swarms of Antarctica. In HALLS, H.C. & FAHRIG, W.F., eds. *Mafic dyke swarms*. Special Paper of the Geological Association of Canada, No. 34, 419-432.
- THOMPSON, R.N. 1982. Magmatism of the British Tertiary province. *Scottish Journal of Geology*, **18**, 49-107.